

RESEARCH ARTICLE

Efficient photocatalytic desulfurization of thiophene under visible light irradiation over flower-like AgBiS₂ photocatalyst

Mehdi Mousavi-Kamazani^{1,*}, Reza Rahmatolahzadeh², Hassan Najafian³

¹ New Technology Faculty, Semnan University, Semnan, Iran

² Polymer Chemistry Department, School of Science, Tehran University, Tehran, Iran

³ Department of Chemistry, Iran University of Science and Technology, Tehran

ARTICLE INFO

Article History:

Received 2020-03-09

Accepted 2020-06-02

Published 2020-10-01

Keywords:

AgBiS₂ nanostructures
Polyol

Photocatalytic

Desulfurization

Radical trapping

ABSTRACT

Here, we report the production of hierarchical flower-like AgBiS₂ nanostructures by an amino acid-modified polyol route. This work indicates that by changing the polyol process conditions including kind of capping agent, reaction time and reflux temperature, the sheet-like, cone-like, sphere-like and flower-like morphologies of AgBiS₂ micro/nanostructures can be prepared. The phase, elemental composition, morphology and optical characteristics of as-prepared AgBiS₂ nanostructures were analyzed by UV-Vis, FESEM, XRD, and EDS techniques. After characterization of the products, the AgBiS₂ nanostructures were employed as novel photocatalysts for oxidative desulfurization of thiophene/n-octane solution as model fuel under visible light illumination. Results demonstrate that hierarchical flower-like AgBiS₂ photocatalyst with desirable band gap energy (2.44 eV) has high photocatalytic desulfurization performance of about 89% after 2 h of visible light irradiation. As well as, the effects of morphology, photocatalyst dosage and reusability of the AgBiS₂ nanostructures on the photocatalytic performance were evaluated. The excellent photocatalytic activity of AgBiS₂ photocatalyst can be attributed to the strong visible light absorption, high separation rate of electron-hole pairs, special hierarchical structures and suitable band gap energy. Moreover, a reliable photo-oxidation desulfurization mechanism was discussed according to the active species trapping experiments, which revealed the photo-generated h⁺ and [•]O₂⁻ radicals were the main active species in the photocatalytic desulfurization process.

How to cite this article

Mousavi-Kamazani M., Rahmatolahzadeh R., Najafian H. Efficient photocatalytic desulfurization of thiophene under visible light irradiation over flower-like AgBiS₂ photocatalyst. J. Nanoanalysis., 2020; 7(4): -13. DOI: 10.22034/jna.***

INTRODUCTION

The critical weather problems arising from atmosphere pollutions have gained extensive attentions, especially the ignition of sulfur-containing gasoline fuels in the automobile engines, which causes the release of extraordinary amounts of sulfur oxides (SO_x) into the air. These harmful compounds seriously threaten the plants, animals and human health [1-3]. Hence, many countries have investigated the diverse desulfurization processes, which can produce “zero” sulfur fuels, including hydrodesulfurization, adsorption desulfurization, biodesulfurization, catalytic desulfurization, oxidative desulfurization,

extraction desulfurization, alkylation and sono-hybrid techniques [4-10]. Among them, the photo-oxidative desulfurization (PODS) route as one of the potential methods for the ultra-deep desulfurization of fuels has received widespread attentions because of the benefits of using the sunlight sources, performance under moderate conditions (low temperature and pressure), using air or H₂O₂ as oxidant, non-use of H₂, high-yield and selectivity, affordable and eco-friendly [1-3, 9-12]. As well known, in the photocatalytic desulfurization process, photocatalyst plays the main role for the oxidation reactions of sulfur atoms to sulfoxides and sulfones [1, 13]. For this reason, preparation of efficient nanophotocatalysts

* Corresponding Author Email: M.Mousavi@semnan.ac.ir

with the suitable band gap in visible light range, low recombination value of electron-hole pairs, and good stability is essential for the ultra-deep desulfurization process.

In recent years, photocatalytic nanomaterials have attracted extensive considerations due to their applications in various environmental and industrial areas, including solar cells, water treatment, oxidation reactions, desulfurization, catalysis, photocatalysis, etc. In a general photocatalysis process, a photocatalyst with the use of solar photons can produce electron-hole (e^-h^+) pairs and subsequently generate powerful active species which can oxidize the organic compounds. However, the traditional photocatalysts suffer from their wide band gaps and high recombination of charge carriers, which only excited under UV illumination. Hence, many efforts have been made to fabricate nanoscale photocatalysts with appropriate band gaps for the effective absorption of visible light radiation to eliminate the environmental pollutants [14-20].

In the last few decades, silver bismuth sulfide ($AgBiS_2$) compounds belonging to I-V-VI group ternary chalcogenides have attracted extensive interest due to their excellent properties in thermoelectric, optoelectronic, optical recording, photoconductivity, dielectric constant, magnetic, and especially in visible light absorption [21-26]. Because of such features, $AgBiS_2$ semiconductors have been widely employed as electrodes or sensitizers in solar cells, catalysts for polymerization of alkylsilanes, photovoltaic absorbers, materials for optoelectronic and thermoelectric devices, and photocatalysts for hydrogen evolution and degradation of Doxycycline [24-29]. Moreover, $AgBiS_2$ nanocrystals possess energy band gap of ~ 1.2 eV, high absorption coefficient of $\alpha = \sim 105$ cm^{-1} (at $\lambda = 600$ nm), earth-abundance and non-toxicity, which make them as good potential candidates for visible-light-driven photocatalytic applications [23, 30, 31]. Moreover, it is well known that the hierarchical micro/nanostructures exhibit interesting features including favorable optical properties, high specific surface area, impressive charge carriers separation, plentiful transport paths for e^-h^+ pairs, superior photocatalytic performance and reusability [32-35]. Hence, adopting an efficient approach for the preparation of hierarchical architectures in nanoscale building is important. So far, several methods have been reported for the synthesis of $AgBiS_2$ structures with various morphologies including microwave, solid-

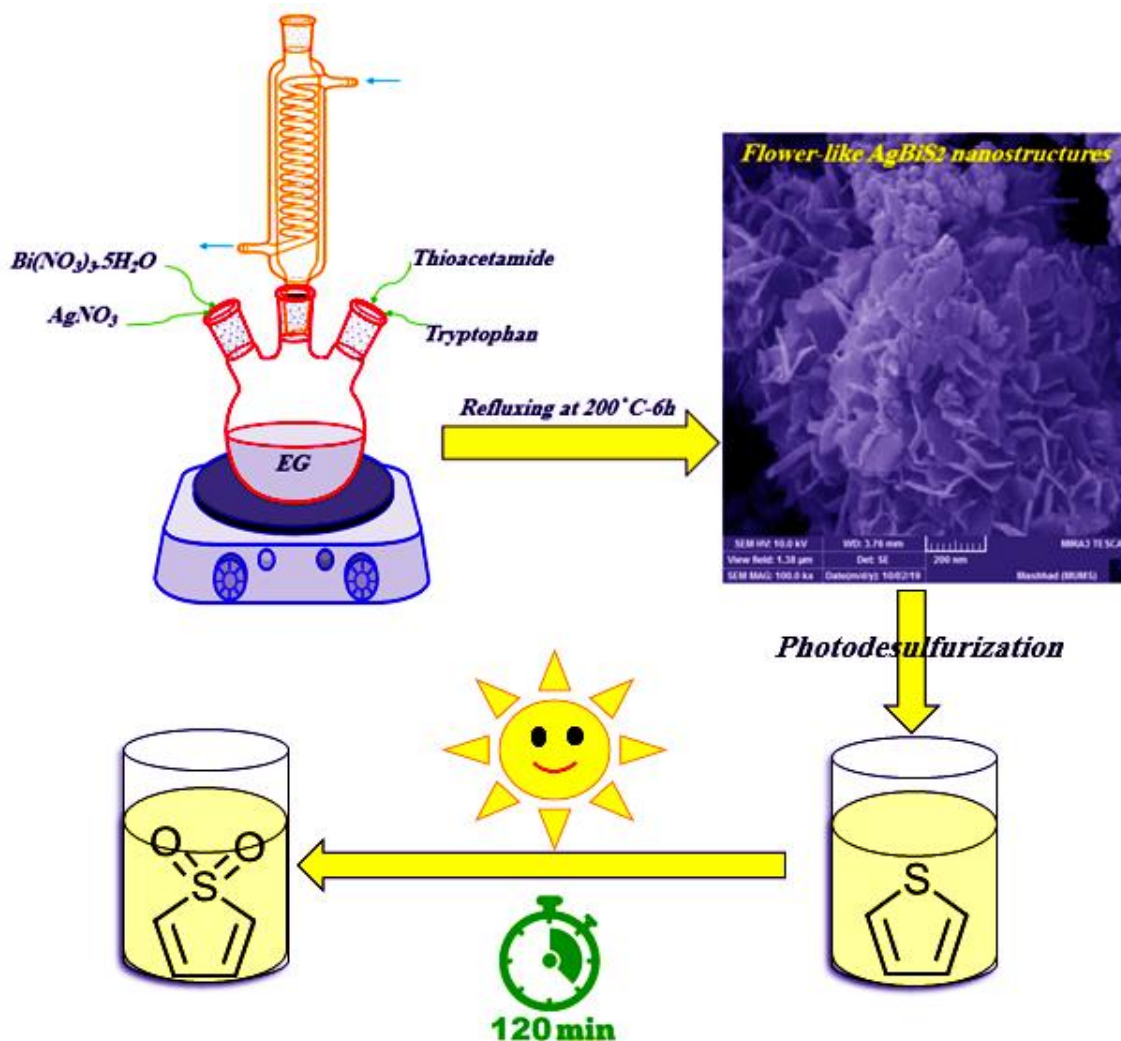
state reaction, hydro/solvothermal, sonochemical, biomolecule-assisted synthesis, template, hot-injection, and polyol route [21, 22, 27, 36-40]. Among these approaches, the polyol technique with benefits like less-energy demanding, simplicity, effectiveness, low-temperature, versatility and environmentally friendly has proved very attractive process for the preparation of nanoscale structures [41, 42].

Herein, hierarchical flower-like $AgBiS_2$ nanostructures were prepared by a polyol approach in the presence of various amino acid as capping agent. The results showed that by controlling the process conditions such as kind of capping agent, reaction time and reflux temperature, the porous flower-like $AgBiS_2$ nanostructures can be formed. Furthermore, for the first time, the $AgBiS_2$ nanostructures were applied as novel photocatalysts for the desulfurization of thiophene under visible light illumination. Results indicate that the flower-like $AgBiS_2$ nanostructures have high photocatalytic desulfurization performance (about 89%) after 2 h of visible light irradiation. Also, the photodesulfurization mechanism was described based on the radical trapping experiment. This photocatalyst provides new design strategy and versatile research prospect for application in the photocatalytic oxidation desulfurization.

EXPERIMENTAL

Materials and Equipments

All the reagents used for the fabrication of $AgBiS_2$ nanostructures including $Bi(NO_3)_3 \cdot 5H_2O$, $AgNO_3$, thioacetamide, ethyleneglycol (EG), glutamic acid, tryptophan, glycine, ethylenediaminetetraacetic acid disodium ($EDTA-Na_2$), benzoquinone (BQ), thiophene, n-octane, methanol and ethanol were of analytical grade and purchased from Sigma-Aldrich company. The particle size and shape of the samples were studied by field emission scanning electron microscopy (FE-SEM, Mira3 Tescan) equipped with an energy dispersive X-ray spectroscopy (EDS). The phase and grain size of the samples were determined by X-ray diffraction (XRD) analysis on a Philips-X'PertPro, X-ray diffractometer using $Cu-K\alpha$ radiation ($\lambda = 0.15418$ nm). UV-Vis diffuse reflectance spectra (UV-Vis-DRS) was obtained using a Shimadzu UV-2550 UV-Vis spectrophotometer. The quantity of sulfur in the photo-desulfurized samples was calculated with X-ray fluorescence sulfur meter (Tanaka Scientific RX-360SH).



Scheme 1. Schematic design of the synthesis of flower-like AgBiS_2 nanostructure (sample 3) by refluxing polyol method and its photocatalytic desulfurization performance.

Synthesis of AgBiS_2 nanostructures

In order to synthesize of the AgBiS_2 nanostructures a facile refluxing polyol approach was employed. For this purpose, certain amounts of $\text{Bi}(\text{NO}_3)_3 \cdot 5\text{H}_2\text{O}$ and AgNO_3 (with 1:1 mole ratio) were dissolved in 20 ml of EG under constant magnetic stirring. Then, 10 ml of EG solution of thioacetamide with 1:1:2 mole ratio to Ag:Bi:S was added into the above mixture and process was carried out for 6 h at 200 °C under reflux. After completion of polyol reaction, the precipitates were filtered and washed with deionized water and ethanol to remove the other impurities. After drying

at 60 °C for 6 h, the AgBiS_2 powders were obtained. Scheme 1 shows the schematic synthesis of the AgBiS_2 nanostructures in presence of tryptophan as capping agent (sample no. 3) and its photocatalytic desulfurization performance. Furthermore, the effect of polyol reaction time, capping agent and reflux temperature on the morphology of the AgBiS_2 compounds were examined and the results are shown in Table 1.

Photocatalytic desulfurization experiment

The photocatalytic desulfurization performance of the AgBiS_2 nanostructures was investigated using

Table 1. The polyol reaction conditions for the preparation of the AgBiS₂ samples and their photocatalytic desulfurization efficiencies.

Sample No.	Polyol reaction time (h)	Capping agent	Reflux temperature (°C)	Figure of SEM images	Desulfurization efficiency (%)
1	1	Tryptophan	200	3a	73
2	3	Tryptophan	200	3b	83
3	6	Tryptophan	200	3c	89
4	6	Tryptophan	100	4a	78
5	6	Tryptophan	150	4b	84
6	6	Glutamic acid	200	5a	67
7	6	Glycine	200	5b	71
8	6	-	200	5c	52

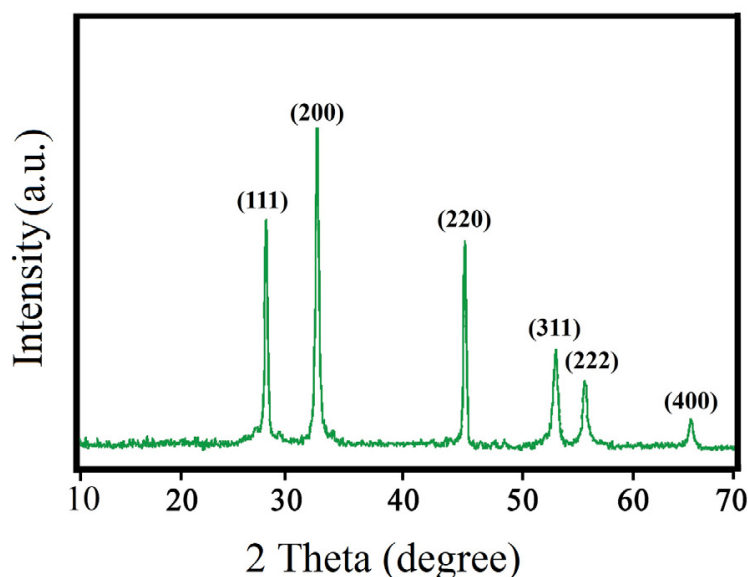


Fig. 1. XRD pattern of the sample 3.

50 mg of the photocatalyst and 50 ml of model fuel (thiophene/n-octane with sulfur content ~ 600 ppm) utilizing visible 400 W Osram lamp. Before the illumination, the suspension was continuously stirred in the dark for 30 min to establish an adsorption/desorption equilibrium and air as oxidant was pumped into the mixture. At certain time intervals, 5 ml of desulfurized solution were withdrawn, centrifuged and then was extracted by methanol as extractant to remove the oxidized thiophene. The desulfurization efficiency (η) of thiophene solution was calculated according to the following formula:

$$\eta = (C_0 - C_t)/C_0 \times 100 \quad (1)$$

where C_0 and C_t are the sulfur concentrations of model fuel for initial and t times, respectively. In addition, to investigate the participating species

in the photocatalytic desulfurization process, radical trapping study was carried out in the same procedure in presence of various kinds of scavengers, such as Na₂-EDTA (as quencher of h⁺) and BQ (as quencher of $\cdot O_2^-$).

RESULTS AND DISCUSSION

The phase purity and composition of the AgBiS₂ nanostructures was studied using X-ray diffraction (XRD) measurement. The XRD pattern (Fig. 1) exhibits that the as-prepared sample no. 3 is cubic phase of AgBiS₂. The main diffraction peaks at 27.2°, 31.7°, 45.4°, 53.8°, 56.4° and 66.1°, are corresponding to (111), (200), (220), (311), (222) and (400) crystal planes, which are in good agreement with the standard JCPDS card No. 21-1178. In addition, there are no characteristic peaks attributable to other impurities, e.g. Ag₂S,

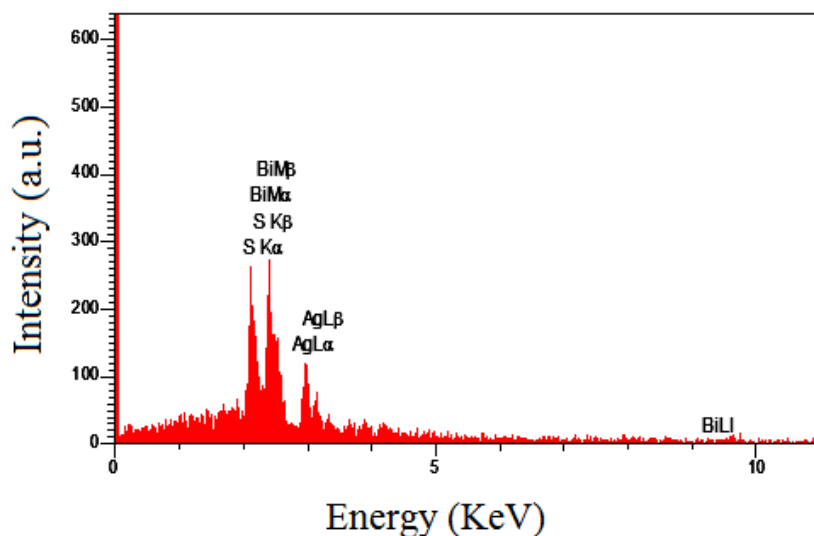


Fig. 2. EDS spectra of the sample 3.

Bi_2S_3 , etc., in the pattern, indicating that the AgBiS_2 products are pure crystalline. The broadening of the peaks demonstrates that the crystalline size of the sample is very small. By using Scherrer formula from the diffraction peaks widths at half maxima, the average diameter of the AgBiS_2 crystals was calculated as ~ 16 nm.

Energy dispersive spectroscopy (EDS) was also applied to determine the elemental composition of the as-synthesized AgBiS_2 nanostructures (sample no. 3). As can be seen in Fig. 2, only the peaks of Ag, Bi, and S elements are present in the EDS spectrum, and the atomic ratio of Ag:Bi:S is 1.04:1.16:2.19, which is close to the stoichiometry of 1:1:2 for AgBiS_2 structures. This result is in good agreement with the result of XRD pattern.

In order to study the effect of the reaction time, capping agent and reflux temperature on the morphology of the AgBiS_2 nanostructures, field emission scanning electron microscopy (FESEM) was used. As shown in Table 1, to examine the influence of the polyol reaction time, the AgBiS_2 samples were prepared for 1 h (sample no. 1), 3 h (sample no. 2) and 6 h (sample no. 3) at 200°C in the presence of tryptophan as capping agent. As seen from the Figs. 3a-c, the reaction time of 1 h, was not enough to form the flower-like nanostructures. In this time, initial agglomerated particles of AgBiS_2 were formed (Fig. 3a). By prolonging the reaction time to 3 h, very fine sheet-like structures were prepared (Fig. 3b). It seems that, by increasing the

reaction time to 3 h, primary particles had enough time to stick together and form the nanosheets. When the refluxing time was extended more to 6 h, nanosheets had enough time to orientated attachment growth and finally the uniform flower-like nanostructures were obtained (Fig. 3c).

Moreover, the effect of the reflux temperature on the size and shape of the AgBiS_2 samples was investigated. For this purpose, polyol process was performed at 100°C (sample no. 4) and 150°C (sample no. 5) for 6 h. As seen in Fig. 4a, at 100°C , the intertwined sheet structures were obtained. Whereas, by increasing the reaction temperature to 150°C , non-assembled sheet-like nanostructures were formed (Fig. 4b). A possible formation mechanism of flower-like AgBiS_2 nanostructures can be proposed. First, the thioacetamide complexes with Ag and Bi ions were formed under the reflux conditions. Second, the as-obtained complexes undergo thermal decomposition at optimum reaction temperature and time. Third, in the presence of the capping agent, the orientation growth of AgBiS_2 nanosheets was carried out in the nucleation and growth stages [22, 41, 43]. Finally, the hierarchical flower-like AgBiS_2 nanostructures aggregated from a large number of nanosheets were prepared.

Furthermore, the AgBiS_2 nanostructures were synthesized by various capping agents including glutamic acid (sample no. 6), glycine (sample no. 7) and tryptophan (sample no. 3), and in the

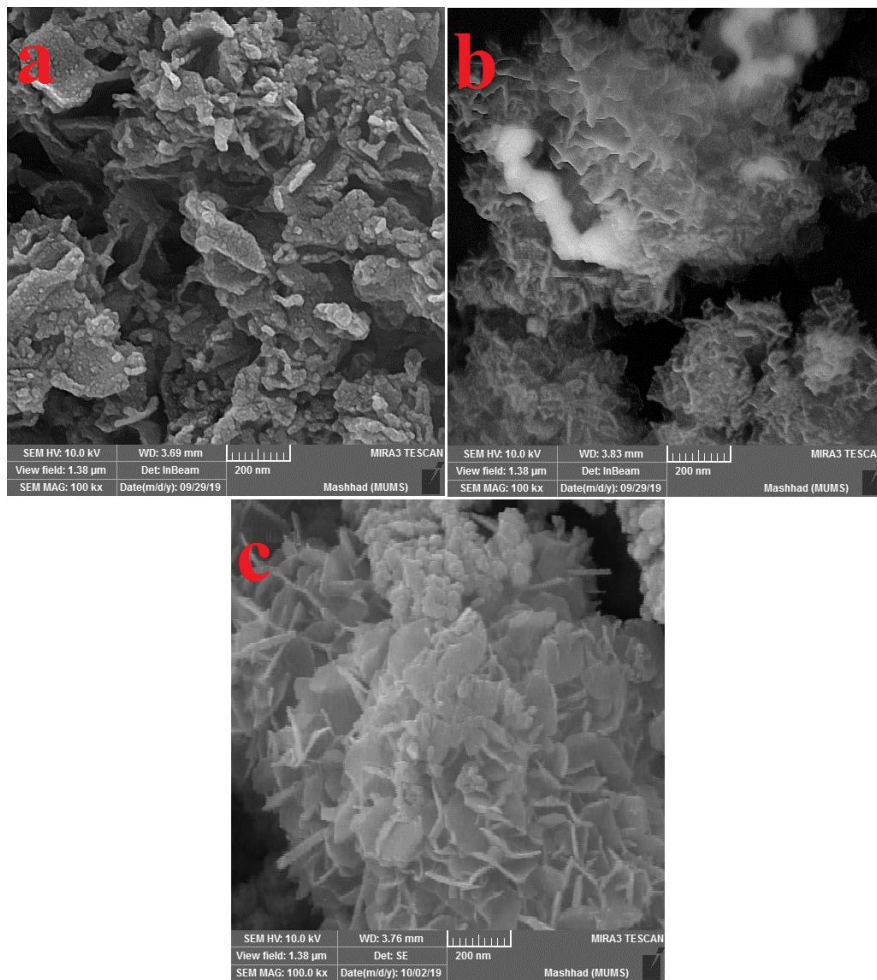


Fig. 3. FESEM images of the (a) sample 1, (b) sample 2 and (c) sample 3, synthesized in different reaction times.

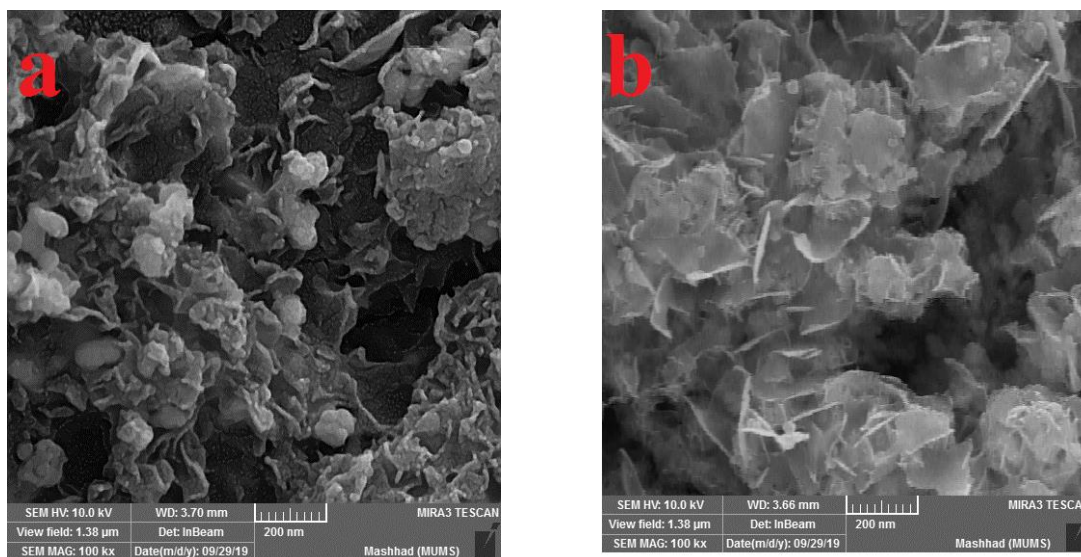


Fig. 4. FESEM images of the (a) sample 4 and (b) sample 5, synthesized at different reaction temperatures.

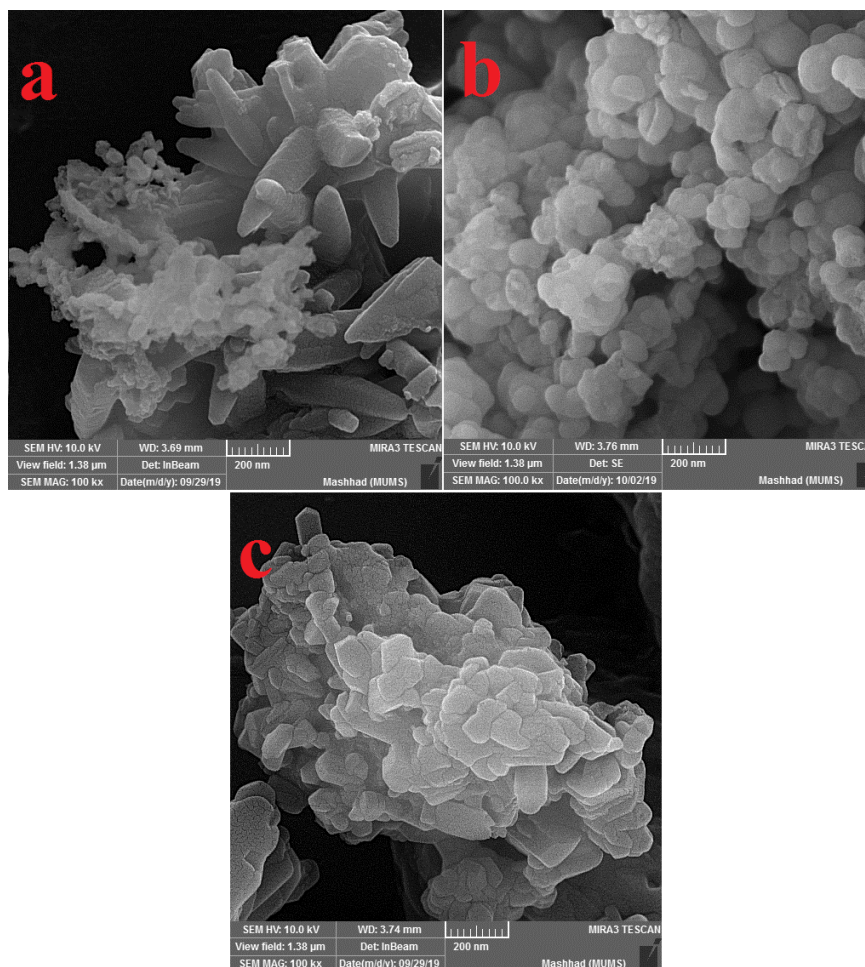


Fig. 5. FESEM images of the (a) sample 6, (b) sample 7 and (c) sample 8, synthesized with different capping agents.

absence of any capping agent (sample no. 8) at 200 °C for 6 h. It can be clearly seen from Figs. 5a-c, that the non-uniform cone-like structures (Fig. 5a), irregular sphere-like nanostructures (Fig. 5b), flower-like nanostructures (Fig. 3c) and agglomerated microstructures (Fig. 5c) were prepared in the presence of the glutamic acid, glycine, tryptophan and without using of capping agent, respectively. These amino acids with various spatial arrangements, can play the role of capping agents. It can be concluded that tryptophan with the highest steric hindrance effect can provide an oriented growth pathway to formation of flower-like AgBiS₂ nanostructures [44].

The light absorption property of the as-fabricated AgBiS₂ nanocrystals was studied by UV-Vis diffuse reflectance spectroscopy (UV-Vis DRS). The DRS spectra of the AgBiS₂ semiconductor (sample no. 3) has been illustrated in Fig. 6a. It can be seen that

a broad and strong peak ranging from 200 to 700 nm has appeared. Specially, it shows a continuous absorption spectrum in the whole visible light area. Thus, the amount of photo-generated charge carriers in the AgBiS₂ photocatalyst can further augmented, which leads to increase the catalytic yield under visible light illumination. Furthermore, the sample has an absorption peak located at 410 nm in wavelength, which compared to the absorption band of the bulk AgBiS₂ (~1050 nm) exhibits a large blue-shift, due to the very small crystalline size of the nanostructures [37]. Commonly, the gap energy (*E_g*) of the crystalline semiconductors can be computed based on the following equation:

$$\alpha h\nu = A(h\nu - E_g)^2 \quad (2)$$

where α is the absorption coefficient, $h\nu$ is the photonic energy, and A is energy-independent constant. The energy band-gap of the product was

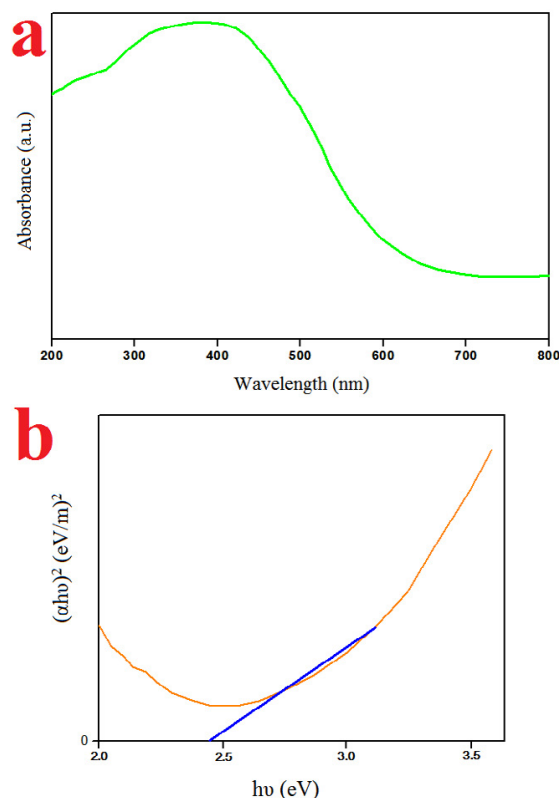
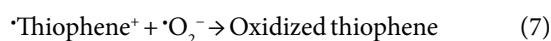
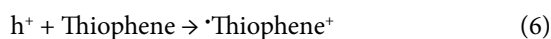


Fig. 6. UV-Vis diffuse reflectance spectrum of the (a) sample 3 and (b) the plot of $(\alpha h\nu)^2$ against $h\nu$ to determine the band gap of the sample 3.

calculated by the Tauc plot of $(\alpha h\nu)^2$ versus $(h\nu)$. The E_g value of the sample no. 3 was determined to be 2.44 eV (Fig. 6b), which is in agreement with the band gap of the reported value [24]. Therefore, it is obvious that the AgBiS_2 nanostructures can be applied as a potential photocatalyst in the visible region.

The catalytic oxidative desulfurization activity of the AgBiS_2 nanostructures was studied by monitoring the photo-oxidation of thiophene/n-octane solution as model fuel using O_2 as the oxidant and methanol as extraction solvent under visible light irradiation. Up to now, the desulfurization performance of the AgBiS_2 compound has not been reported. The blank experiments showed that in the absence of AgBiS_2 photocatalyst or visible light irradiation, thiophene molecules could not be oxidized (Fig. 7a), that indicated the oxidation process was mainly due to photocatalytic reactions. As illustrated in the Table 1, the results exhibited that the sample no. 3 with particular morphology has better desulfurization efficiency about 89% after 2 h of visible light irradiation (Fig. 7a). The proposed

mechanism of photocatalytic desulfurization process of the AgBiS_2 nanostructures is shown by the following equations [12, 45]:



As shown in Scheme 2, the AgBiS_2 can adsorb the photons and instantly produce the electrons and holes on its conduction band (CB) and valance band (VB), respectively. Afterward, the electrons accumulated in the CB can react with O_2 molecules and generate reactive oxygen anion superoxide ($\cdot\text{O}_2^-$). These oxidative radicals can attack to the sulfur atoms in the thiophene and generate the oxidized compounds. Simultaneously,

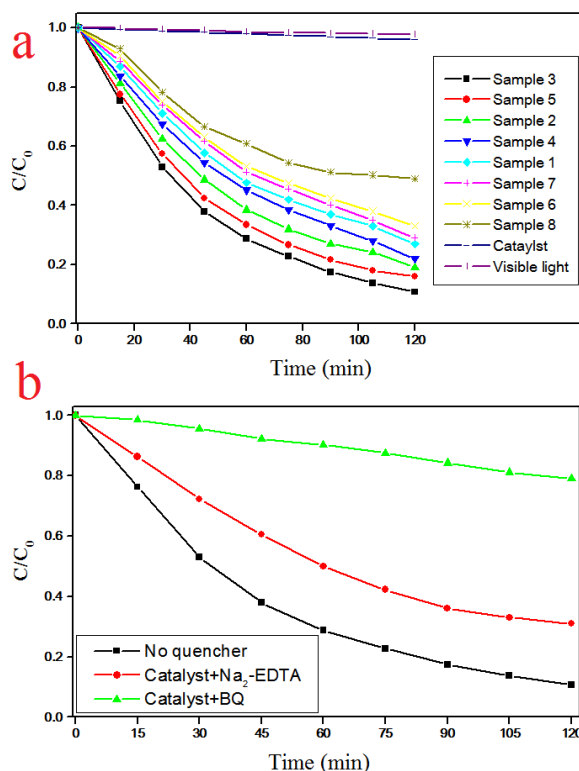
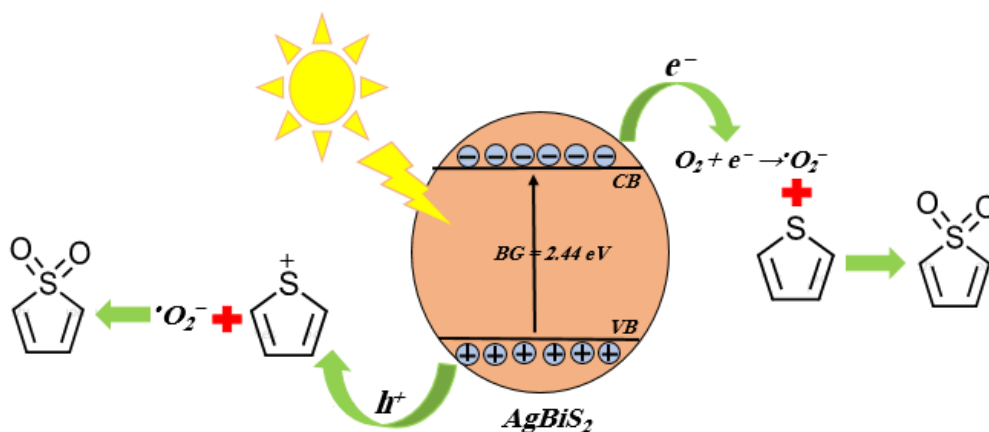


Fig. 7. (a) Photodesulfurization curves of thiophene over samples 1-8 under visible light illumination and (b) trapping experiment of active species during the photocatalytic desulfurization over AgBiS_2 nanostructure (sample 3) by using different quenchers.



Scheme 2. Schematic mechanism for the oxidation of thiophene by photogenerated electron-hole pairs in AgBiS_2 nanostructure.

thiophene can combine with the holes (h^+) to form 'thiophene⁺', which is then oxidized by active $\cdot\text{O}_2^-$ radicals [4, 46]. The excellent photocatalytic performance of the AgBiS_2 nanostructures can be ascribed to the lower charge carrier recombination, appropriate band gap energy and more active sites of the photocatalyst [1, 47].

Moreover, to further revelation the photocatalytic desulfurization mechanism of flower-like AgBiS_2 nanostructures, the radical trapping experiment was employed to characterize the contributor active species in the desulfurization process. It is well known that the superoxide radical ($\cdot\text{O}_2^-$) and hole (h^+) were generally considered as

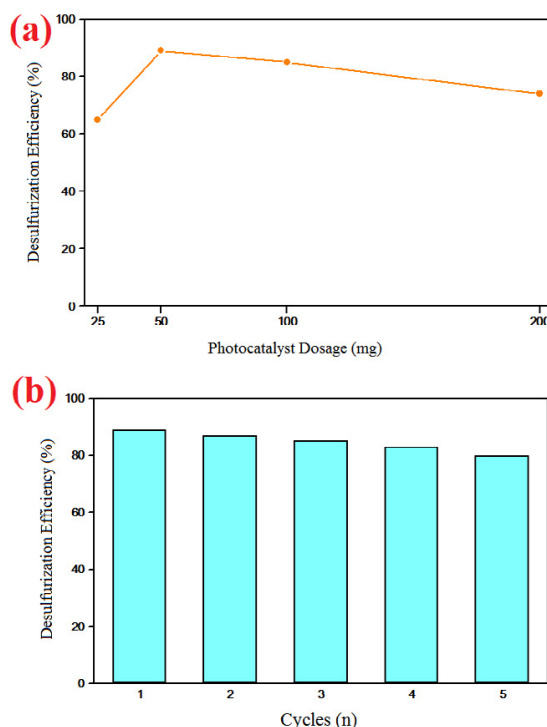


Fig. 8. (a) the effect of photocatalyst dosage on the photodesulfurization efficiency of the AgBiS_2 nanostructure (sample 3) and (b) the recyclability of the sample 3 for 5 cycles of photocatalytic desulfurization reaction.

the basic species in the photocatalytic reactions [48, 49]. Hence, the radical trapping was performed utilizing BQ and $\text{Na}_2\text{-EDTA}$ as the scavengers of superoxide radical ($\cdot\text{O}_2^-$) and hole (h^+), respectively. As shown in Fig. 7b, the benzoquinone notably repressed the photo-desulfurization process performance, whilst by adding the $\text{Na}_2\text{-EDTA}$, the desulfurization efficiency partially decreased. The amount of desulfurization efficiency was reduced from 89% to 21% and 69% in the presence of BQ and $\text{Na}_2\text{-EDTA}$, respectively. Therefore, this result suggested that the photo-generated superoxide radicals ($\cdot\text{O}_2^-$) has played the main role in the photocatalytic desulfurization of thiophene by AgBiS_2 nanostructures.

To examine the effect of AgBiS_2 photocatalyst dosage on the photocatalytic desulfurization efficiency, the values of 25, 50, 100 and 200 mg from the sample no. 3 were applied in desulfurization of thiophene solution (600 ppm) under 2 h of visible light irradiation. The photodesulfurization efficiency of thiophene in each amount of photocatalyst were approximate 65, 89, 85 and 74%, respectively. As shown in Fig. 8a, by adding the photocatalyst loading from 25 to 50 mg, due

to the increase in the number of surface active sites and interactions, the desulfurization rate of thiophene was enhanced. Whereas, by further boosting in photocatalyst dosage to 100 and 200 mg, due to the high accumulation of nanoparticles and then decrement in surface active sites on the photocatalyst, the desulfurization performance of AgBiS_2 was reduced [50, 51].

In the industrial applications, the recovery and reusability of the catalysts is economically valuable. Therefore, the recyclability of the flower-like AgBiS_2 nanostructures (sample no. 3) was carried out for 5 runs of desulfurization experiment. From Fig. 8b, it is obvious that even after 5 recycles, the photocatalytic activity remained constant, which indicates that the AgBiS_2 nanostructure can be employed as a recyclable photocatalyst for the photocatalytic applications under sun light irradiation.

CONCLUSIONS

In the present study, hierarchical flower-like AgBiS_2 nanostructures have been synthesized by an amino acid-modified refluxing polyol process. We found that sheet-like, cone-like, sphere-

like and flower-like morphologies of the AgBiS₂ nanostructures can be achieved by controlling the reaction parameters including type of capping agent, reaction time and reflux temperature. Finally, we employed the AgBiS₂ photocatalysts with different morphologies to desulfurize the thiophene as model fuel in the presence of O₂ as oxidant and methanol as extraction solvent under visible light illumination. Results illustrate that the hierarchical flower-like AgBiS₂ photocatalyst with suitable band gap energy (~2.44 eV) has good photocatalytic desulfurization activity (~89%) after 2h of visible light irradiation. Also, the impacts of morphology, catalyst dosage and recyclability of the AgBiS₂ products on the photocatalytic efficiency were examined. The superior photocatalytic performance of AgBiS₂ photocatalyst can be ascribed to the good visible photon absorption, high separation efficiency of charge carriers, particular hierarchical structures and appropriate band gap energy. Moreover, the reliable photocatalytic mechanism was suggested according to the active species trapping experiments, which showed the photo-induced h⁺ and •O₂⁻ species were the dominant active species in the photocatalytic oxidative desulfurization process. The superior efficiency, low-cost, and simple synthesis of AgBiS₂ proves its promising potential for photodesulfurization applications.

ACKNOWLEDGEMENTS

Authors are grateful to the council of Iran National Science Foundation (INSF) and University of Semnan for supporting this work.

CONFLICT OF INTEREST

The authors declare that they have no known competing financial interests or personal relationships that could have appeared to influence the work reported in this paper.

REFERENCES

1. Mostafa MM, El saied M, Morshedy AS. Novel Calcium Carbonate-titania nanocomposites for enhanced sun light photo catalytic desulfurization process. *Journal of Environmental Management*. 2019;250:109462.
2. Guo L, Zhao Q, Wang C, Shen H, Han Xa, Zhang K, et al. Magnetically recyclable Fe₃O₄@SiO₂/Bi₂WO₆/Bi₂S₃ with visible-light-driven photocatalytic oxidative desulfurization. *Materials Research Bulletin*. 2019;118:110520.
3. I.V. Babichi, J.A. Moulijn, Science and technology of novel processes for deep desulfurization of oil refinery streams: a review, *Fuel*, 82 (2003) 607–631.
4. Wang L, Cai H, Li S, Mominou N. Ultra-deep removal of thiophene compounds in diesel oil over catalyst TiO₂/Ni-ZSM-5 assisted by ultraviolet irradiating. *Fuel*. 2013;105:752-6.
5. Padilha CEa, Dantas PVF, Sousa Júnior FC, Oliveira Júnior SD, Nogueira CdC, Souza DFdS, et al. Recovery and concentration of ortho-phenylphenol from biodesulfurization of 4-methyl dibenzothiophene by aqueous two-phase flotation. *Separation and Purification Technology*. 2017;176:306-12.
6. Sun X, Tatarchuk BJ. Photo-assisted adsorptive desulfurization of hydrocarbon fuels over TiO₂ and Ag/TiO₂. *Fuel*. 2016;183:550-6.
7. Ahmed Rahma WS, Mjalli FS, Al-Wahaibi T, Al-Hashmi AA. Polymeric-based deep eutectic solvents for effective extractive desulfurization of liquid fuel at ambient conditions. *Chemical Engineering Research and Design*. 2017;120:271-83.
8. Zheng H, Sun Z, Chen X, Zhao Q, Wang X, Jiang Z. A micro reaction-controlled phase-transfer catalyst for oxidative desulfurization based on polyoxometalate modified silica. *Applied Catalysis A: General*. 2013;467:26-32.
9. Li S, Mominou N, Wang Z, Liu L, Wang L. Ultra-deep Desulfurization of Gasoline with CuW/TiO₂-GO through Photocatalytic Oxidation. *Energy & Fuels*. 2016.
10. Bhasarkar JB, Chakma S, Moholkar VS. Investigations in physical mechanism of the oxidative desulfurization process assisted simultaneously by phase transfer agent and ultrasound. *Ultrasonics Sonochemistry*. 2015;24:98-106.
11. Lei W, Wenya W, Mominou N, Liu L, Li S. Ultra-deep desulfurization of gasoline through aqueous phase in-situ hydrogenation and photocatalytic oxidation. *Applied Catalysis B: Environmental*. 2016;193:180-8.
12. Cai Y, Song H, An Z, Xiang X, Shu X, He J. The confined space electron transfer in phosphotungstate intercalated ZnAl-LDHs enhances its photocatalytic performance for oxidation/extraction desulfurization of model oil in air. *Green Chemistry*. 2018;20(24):5509-19.
13. Gao H, Guo C, Xing J, Zhao J, Liu H. Extraction and oxidative desulfurization of diesel fuel catalyzed by a Brønsted acidic ionic liquid at room temperature. *Green Chemistry*. 2010;12(7):1220.
14. Mousavi-Kamazani M, Rahmatolahzadeh R, Amin Shobeiri S, Beshkar F. Sonochemical synthesis, formation mechanism, and solar cell application of tellurium nanoparticles. *Ultrasonics Sonochemistry*. 2017;39:233-9.
15. Shobeiri SA, Mousavi-Kamazani M, Beshkar F. Facile mechanical milling synthesis of NiCr₂O₄ using novel organometallic precursors and investigation of its photocatalytic activity. *Journal of Materials Science: Materials in Electronics*. 2017;28(11):8108-15.
16. Mousavi-Kamazani M, Rahmatolahzadeh R, Beshkar F. Facile Solvothermal Synthesis of CeO₂-CuO Nanocomposite Photocatalyst Using Novel Precursors with Enhanced Photocatalytic Performance in Dye Degradation. *Journal of Inorganic and Organometallic Polymers and Materials*. 2017;27(5):1342-50.
17. Mousavi-Kamazani M. Facile sonochemical-assisted synthesis of Cu/ZnO/Al₂O₃ nanocomposites under vacuum: Optical and photocatalytic studies. *Ultrasonics Sonochemistry*. 2019;58:104636.
18. Mousavi-Kamazani M. Facile hydrothermal synthesis of egg-like BiVO₄ nanostructures for photocatalytic desulfurization of thiophene under visible light irradiation.

- Journal of Materials Science: Materials in Electronics. 2019;30(19):17735-40.
19. Mousavi-Kamazani M, Zarghami Z, Rahmatolahzadeh R, Ramezani M. Solvent-free synthesis of Cu-Cu₂O nanocomposites via green thermal decomposition route using novel precursor and investigation of its photocatalytic activity. *Advanced Powder Technology*. 2017;28(9):2078-86.
 20. Mousavi-Kamazani M, Salavati-Niasari M, Ramezani M. Preparation and Characterization of Cu₂S Nanoparticles Via Ultrasonic Method. *Journal of Cluster Science*. 2012;24(3):927-34.
 21. Bernechea M, Miller NC, Xercavins G, So D, Stavrinadis A, Konstantatos G. Solution-processed solar cells based on environmentally friendly AgBiS₂ nanocrystals. *Nature Photonics*. 2016;10(8):521-5.
 22. Chen D, Shen G, Tang K, Jiang X, Huang L, Jin Y, et al. Microwave synthesis of AgBiS₂ dendrites in aqueous solution. *Inorganic Chemistry Communications*. 2003;6(6):710-2.
 23. Huang P-C, Yang W-C, Lee M-W. AgBiS₂ Semiconductor-Sensitized Solar Cells. *The Journal of Physical Chemistry C*. 2013;117(36):18308-14.
 24. Liang N, Chen W, Dai F, Wu X, Zhang W, Li Z, et al. Homogeneously hexagonal prismatic AgBiS₂ nanocrystals: controlled synthesis and application in quantum dot-sensitized solar cells. *CrystEngComm*. 2015;17(9):1902-5.
 25. Chen C, Qiu X, Ji S, Jia C, Ye C. The synthesis of monodispersed AgBiS₂ quantum dots with a giant dielectric constant. *CrystEngComm*. 2013;15(38):7644.
 26. Ganguly P, Mathew S, Clarizia L, Kumar R S, Akande A, Hinder S, et al. Theoretical and experimental investigation of visible light responsive AgBiS₂-TiO₂ heterojunctions for enhanced photocatalytic applications. *Applied Catalysis B: Environmental*. 2019;253:401-18.
 27. Wang J, Yang X, Hu W, Li B, Yan J, Hu J. Synthesis of AgBiS₂ microspheres by a templating method and their catalytic polymerization of alkylsilanes. *Chemical Communications*. 2007(46):4931.
 28. Oh JT, Bae SY, Ha SR, Cho H, Lim SJ, Boukhvalov DW, et al. Water-resistant AgBiS₂ colloidal nanocrystal solids for eco-friendly thin film photovoltaics. *Nanoscale*. 2019;11(19):9633-40.
 29. Thongtem T, Tipcompor N, Thongtem S. Characterization of AgBiS₂ nanostructured flowers produced by solvothermal reaction. *Materials Letters*. 2010;64(6):755-8.
 30. Hu L, Patterson RJ, Zhang Z, Hu Y, Li D, Chen Z, et al. Enhanced optoelectronic performance in AgBiS₂ nanocrystals obtained via an improved amine-based synthesis route. *Journal of Materials Chemistry C*. 2018;6(4):731-7.
 31. Manimozhi T, Archana J, Navaneethan M, Ramamurthi K. Shape-controlled synthesis of AgBiS₂ nano-/microstructures using PEG-assisted facile solvothermal method and their functional properties. *Applied Surface Science*. 2019;487:664-73.
 32. Namvar F, Beshkar F, Salavati-Niasari M, Bagheri S. Morphology-controlled synthesis, characterization and photocatalytic property of hierarchical flower-like Dy₂Mo₃O₉ nanostructures. *Journal of Materials Science: Materials in Electronics*. 2017;28(14):10313-20.
 33. Valian M, Beshkar F, Salavati-Niasari M. Urchin-like Dy₂CoMnO₆ double perovskite nanostructures: new simple fabrication and investigation of their photocatalytic properties. *Journal of Materials Science: Materials in Electronics*. 2017;28(17):12440-7.
 34. Beshkar F, Salavati-Niasari M, Amiri O. Superhydrophobic-superoleophilic copper-graphite/styrene-butadiene-styrene based cotton filter for efficient separation of oil derivatives from aqueous mixtures. *Cellulose*. 2020;27(8):4691-705.
 35. Panahi-Kalamuei M, Mousavi-Kamazani M, Salavati-Niasari M. Self-assembly of nanoparticles to form tree-like tellurium nanostructures using novel starting reagents. *Materials Letters*. 2014;136:218-21.
 36. Bryndzia LT, Kleppa OJ. Standard enthalpies of formation of sulfides and sulfosalts in the Ag-Bi-S system by high-temperature, direct synthesis calorimetry. *Economic Geology*. 1988;83(1):174-81.
 37. Zhong J, Xiang W, Xie C, Liang X, Xu X. Synthesis of spheroidal AgBiS₂ microcrystals by L-cysteine assisted method. *Materials Chemistry and Physics*. 2013;138(2-3):773-9.
 38. Xie B, Yuan S, Jiang Y, Lu J, Li Q, Wu Y, et al. Molecular Template Preparation of AgBiS₂ Nanowhiskers. *Chemistry Letters*. 2002;31(6):612-3.
 39. Pejova B, Grozdanov I, Nesheva D, Petrova A. Size-Dependent Properties of Sonochemically Synthesized Three-Dimensional Arrays of Close-Packed Semiconducting AgBiS₂ Quantum Dots. *Chemistry of Materials*. 2008;20(7):2551-65.
 40. Liu H, Zhong J, Liang X, Zhang J, Xiang W. A mild biomolecule-assisted route for preparation of flower-like AgBiS₂ crystals. *Journal of Alloys and Compounds*. 2011;509(27):L267-L72.
 41. Shen G, Chen D, Tang K, Qian Y. Novel polyol route to AgBiS₂ nanorods. *Journal of Crystal Growth*. 2003;252(1-3):199-201.
 42. Cai W, Wan J. Facile synthesis of superparamagnetic magnetite nanoparticles in liquid polyols. *Journal of Colloid and Interface Science*. 2007;305(2):366-70.
 43. Shen G, Chen D, Tang K, Huang L, Qian Y. Large-scale synthesis of (Bi₂(Bi₂S₃)₉I₃)_{0.667} submicrometer needle-like crystals via a novel polyol route. *Journal of Crystal Growth*. 2003;249(1-2):331-4.
 44. Najafian H, Manteghi F, Beshkar F, Salavati-Niasari M. Fabrication of nanocomposite photocatalyst CuBi₂O₄/Bi₃ClO₄ for removal of acid brown 14 as water pollutant under visible light irradiation. *Journal of Hazardous Materials*. 2019;361:210-20.
 45. Gao M, Zhang G, Tian M, Liu B, Chen W. Oxidative desulfurization of dibenzothiophene by central metal ions of chlorophthalocyanines-tetracarboxyl complexes. *Inorganica Chimica Acta*. 2019;485:58-63.
 46. Gao H, Wu X, Sun D, Niu G, Guan J, Meng X, et al. Preparation of core-shell PW₁₂@TiO₂ microspheres and oxidative desulfurization performance. *Dalton Transactions*. 2019;48(17):5749-55.
 47. Najafian H, Manteghi F, Beshkar F, Salavati-Niasari M. Enhanced photocatalytic activity of a novel NiO/Bi₂O₃/Bi₃ClO₄ nanocomposite for the degradation of azo dye pollutants under visible light irradiation. *Separation and Purification Technology*. 2019;209:6-17.
 48. Najafian H, Manteghi F, Beshkar F, Salavati-Niasari M. Efficient degradation of azo dye pollutants on ZnBi₃8O₅ nanostructures under visible-light irradiation. *Separation and Purification Technology*. 2018;195:30-6.
 49. Ranjeh M, Beshkar F, Salavati-Niasari M. Sol-gel synthesis of novel Li-based boron oxides nanocomposite for photodegradation of azo-dye pollutant under UV light irradiation.

- Composites Part B: Engineering. 2019;172:33-40.
50. Mousavi-Kamazani M, Ghodrati M, Rahmatolahzadeh R. Fabrication of Z-scheme flower-like AgI/Bi₂O₃ heterojunctions with enhanced visible light photocatalytic desulfurization under mild conditions. *Journal of Materials Science: Materials in Electronics*. 2020;31(7):5622-34.
51. Mousavi-Kamazani M. Cube-like Cu/Cu₂O/BiVO₄/Bi₇VO₁₃ composite nanoparticles: Facile sol-gel synthesis for photocatalytic desulfurization of thiophene under visible light. *Journal of Alloys and Compounds*. 2020;823:153786.